Estimation of Nusselt Number and the First Wall Heat Extraction Capability in Self-Cooled Liquid Metal Blankets

Amit K. Srivastava[1], Abdul B. Ahmad[1] and M. S. Kalra[1]
[1]Nuclear Engineering and Technology Program,
Indian Institute of Technology Kanpur,
Kanpur - 208016, India
Email: msk@iitk.ac.in

Abstract

Self-cooled liquid metal breeding blankets are in principle the simplest type of blankets that can be used in fusion reactors. Two critical issues in such blankets are strong magnetohydrodynamic (MHD) effects and the heat extraction capability from the first wall using liquid metals. In this work we estimate from first principles the MHD friction factors and Nusselt numbers applicable to convective cooling of the first wall using liquid metals. This is followed by a parametric, thermal-hydraulic study of the first wall cooling capability in self-cooled blankets with emphasis on coolant channel dimensions, dynamic pressure drop and heat removal rate to pumping power ratio.

1. Introduction

The realization of controlled thermonuclear fusion can lead to a potentially inexhaustible source of energy. Development of viable blanket systems is one of the essential requirements before the feasibility of fusion as a commercial energy source can be established. In principle, self-cooled liquid metal breeding blankets are the simplest type of blankets that can be used in magnetically confined controlled thermonuclear fusion reactors. Their inherent simplicity arises from the fact that the liquid metal serves both as a coolant and a tritium breeder which simplifies the material and design requirements. Liquid metals have attractive heat transfer and heat removal characteristics and several other potential advantages such as low pressure and high temperature operation, immunity to radiation damage, potential for tritium self-sufficiency and a greater flexibility for tritium removal, etc.

One of the unfavorable features or constraints in self-cooled liquid metal blankets is related to MHD effects. The motion of liquid metals in the strong magnetic field in a fusion reactor blanket induces electric current, interaction of which with the magnetic field results in a Lorentz force opposite to the flow direction. This leads to high MHD pressure drop and pumping power requirement for the heat removal system.

Another critical issue in designing of a self- cooled blanket is the cooling of the first wall which is subjected to intense heat load due to thermal conduction and radiation from plasma. In the present work we have done a parametric study of the first wall cooling capability in self-cooled liquid metal blankets. By solving the coupled induction, linear momentum and temperature equations for a rectangular channel, we first estimate the friction factor and Nusselt number with heat flux applied to one of the side walls. Using these, we assess the channel cross section, pressure drop, and the ratio of heat removal rate to pumping power for the ducts employed for heat extraction from the first wall and show their dependence on major input parameters.

2. Steady State Governing Equations

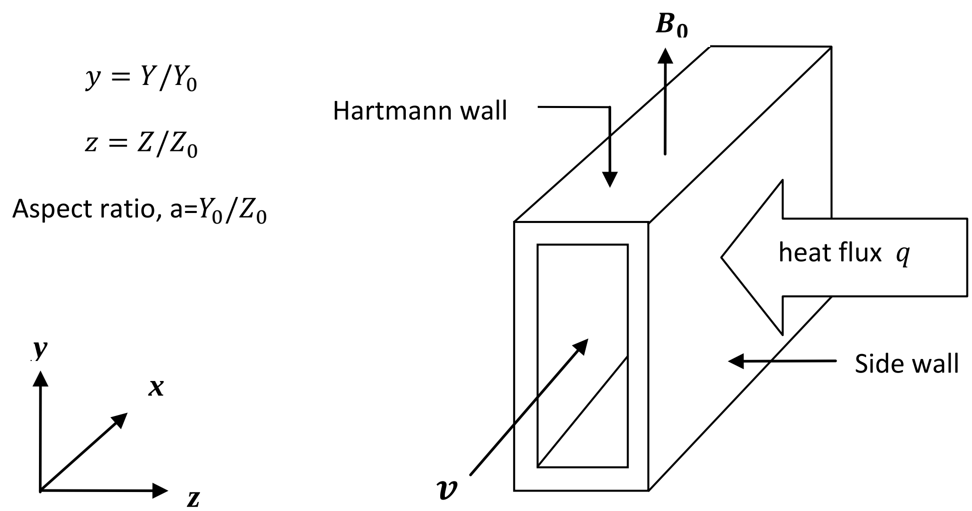

Fig. 1 A schematic sketch of the flow channel (one side wall heating)

We consider a rectangular channel with uniform cross section and electrically insulated side and Hartmann walls as shown in Fig. 1. Uniform heat flux is applied to all or one of the side walls. In the later case the other three walls are thermally insulated. For fully developed flow the governing equations can be written in the following dimensionless form [1, 2]:

Induction equation

$$\frac{\partial^2 b}{\partial y^2} + a^2 \frac{\partial^2 b}{\partial z^2} + H \frac{\partial u}{\partial y} = 0 \tag{1}$$

Linear momentum equation

$$\frac{\partial^2 u}{\partial y^2} + a^2 \frac{\partial^2 u}{\partial z^2} + H \frac{\partial b}{\partial y} = -1 \tag{2}$$

Temperature equation

$$\frac{\partial^2 \theta}{\partial y^2} + a^2 \frac{\partial^2 \theta}{\partial z^2} = \frac{(1+a)u(y,z)}{u_{mean}} \qquad \text{(all sides heated)} \tag{3a}$$

$$= \frac{a u(y,z)}{2u_{mean}} \qquad \text{(one side wall heated)} \tag{3b}$$

where the symbols are given in the Nomenclature. The magnetic field, the velocity, and the temperature are non-dimensionlized as follows:

$$\boldsymbol{b} = b(y,z)\hat{\boldsymbol{x}} = \frac{H}{Rm}(\boldsymbol{B}-\boldsymbol{B_0}), \quad \boldsymbol{u} = u\hat{\boldsymbol{x}} = \frac{\boldsymbol{v}}{v_N}, \quad \theta = \frac{(T_s - T)k}{qY_0} \tag{4}$$

where

$$v_N = -\frac{Y_0^2\left(\frac{dp}{dX}\right)}{\rho\nu} \tag{5}$$

Boundary conditions

For the velocity field, the hydrodynamic boundary condition $u = 0$ at the boundary of the channel is taken. For electrically insulated channel walls, the induced magnetic field $b = 0$ at the walls [1]. At the heated wall(s), $\theta = 0$ and at the insulated wall(s), the first derivative of θ with respect to the normal to the wall is taken as zero.

It may be pointed out here that the temperature equation relevant for the first wall cooling is when one sidewall is heated and the other three walls are insulated. We have, however, also solved the temperature equation with all sides heated to compare the Nusselt number for the two cases and to validate the code by checking the hydrodynamics limits as $H \to 0$.

Furthermore, for the ducts /channels used for cooling the first wall, we ignore the volumetric heat deposition by neutrons as this will be small compared to the intense heat flux from the first wall.

3. Numerical Solution

All numerical computations have been done in MATLAB using both uniform and non-uniform grid with a finer mesh at the boundaries [5]. The later is particularly essential for resolving sharp velocity gradient at the boundaries as Hartmann number H increases. The governing equations are discretized using central differences [6]. For improving computational efficiency we have used the concept of sparse matrices because the resulting matrix is loosely dense. Equations 1 to 3a can be solved over one quadrant of the channel due to symmetry, but Eq. 3b must be solved by discretizing the entire domain. When using only one quadrant of the domain the normal derivatives of u and θ at y or $z = 0$ are equated to zero, whereas the induced magnetic field b is taken zero at $y = 0$, and its normal derivative is put to zero at $z = 0$ [1, 4].

A characteristic dimensionless velocity profile obtained by simultaneously solving Eqs. 1 and 2 with boundary conditions as explained above is shown in Fig. 2 for Hartmann number $H = 50$. Using the computed velocity profile, the temperature profiles are obtained by solving Eq. 3a for uniform heating on all sides of the channel and Eq. 3b for only one of the side walls (normal to the Hartmann walls) being uniformly heated, considering other sides as insulated. These temperature profiles are shown in Figs. 3 and 4, respectively.

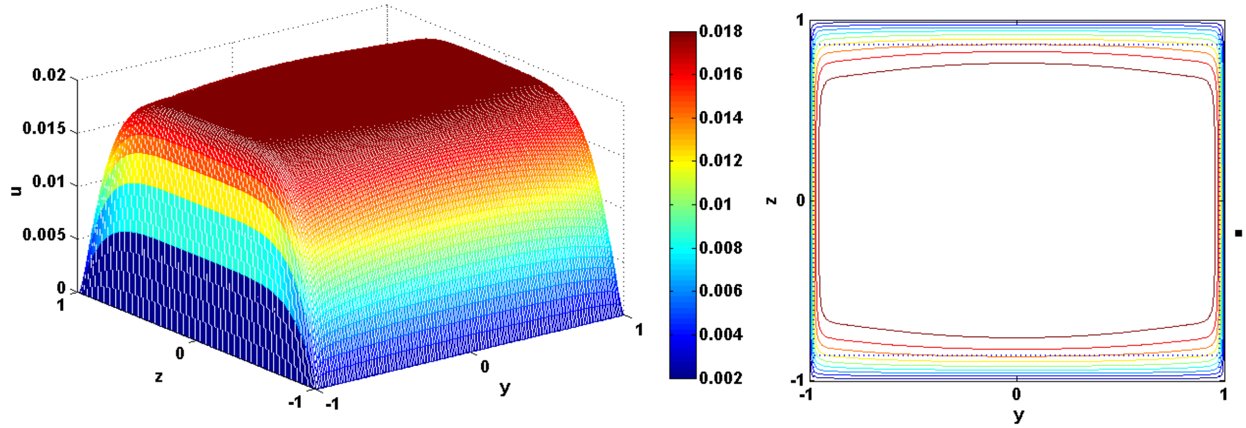

Fig. 2 Dimensionless velocity profile and isolines for Hartmann Number $H = 50$

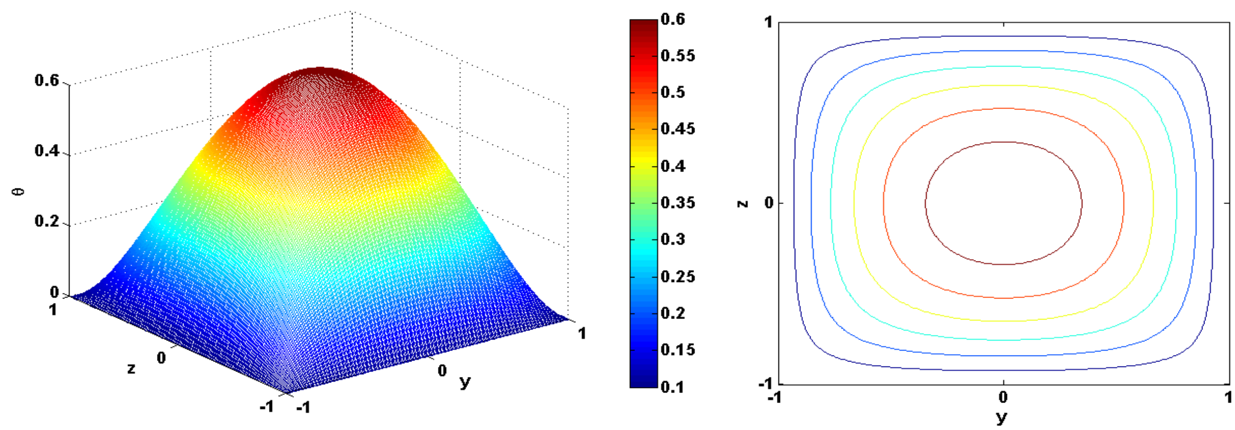

Fig. 3 Dimensionless temperature profile and isolines for all sides heated $(H = 50)$

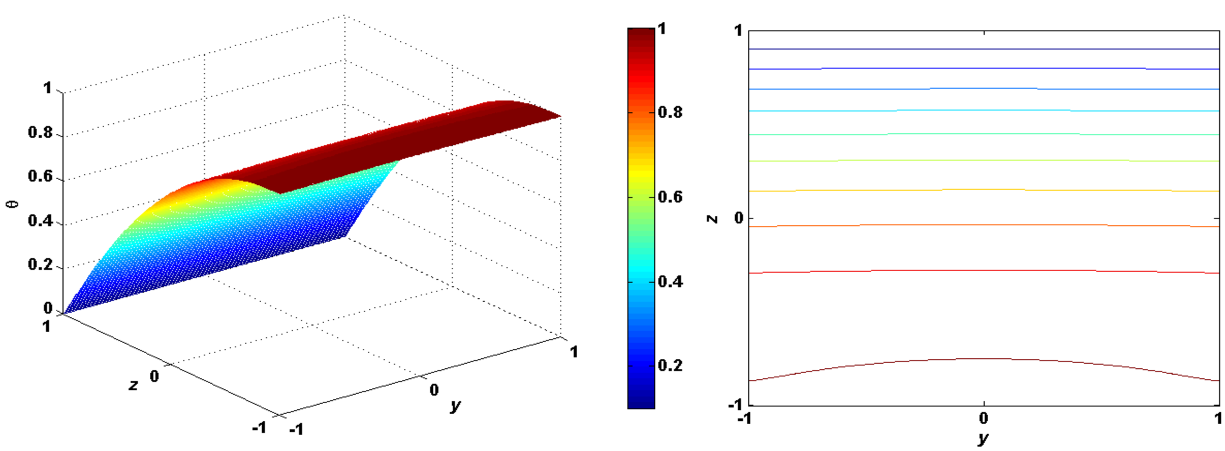

Fig. 4 Dimensionless temperature profile and isolines for one side wall heated for $(H = 50)$

4. Friction Factor and Nusselt Number

From the velocity and temperature profiles, the friction factor and Nusselt number can be obtained. The friction factor, f, is defined as

$$f = -\frac{D\frac{dp}{dX}}{\frac{1}{2}\rho v_{mean}^2}, \qquad D = \frac{4Y_0Z_0}{Y_0 + Z_0} = \frac{4Y_0}{1+a} \ . \tag{6}$$

With the velocity normalization as defined in Eq. 5, it is straight forward to see that

$$fRe = \frac{32}{(1+a)^2 u_{mean}} \tag{7}$$

where symbols are as given in the Nomenclature. The computed value of fRe for Hartmann number upto $H = 400$ are shown in Fig. 5. It can be seen from the figure that the computed values of fRe tend to their hydrodynamic limits as given in literature [2, 4]. Furthermore, it is apparent from Fig. 5 that for $H > 50$ or so, a linear scaling between fRe and H exists for electrically insulated walls:

$$fRe = \chi(a)H \qquad H > 50 \tag{8}$$

The slope $\chi(a)$ depends only on the aspect ratio, a, and can easily be obtained from Fig. 5. It is given in Table 1 for a=1 to 3.

Similarly, from the definition of the Nusselt Number

$$Nu = \frac{hD}{k} \ , \tag{9}$$

where $h = q/(T_s - T_{mean})$ is the convective heat transfer coefficient, and the temperature normalization as in Eq. 4, it can be seen that

$$Nu = \frac{4}{(1+a)\theta_{mean}} \ , \qquad \text{where } \theta_{mean} = \frac{(u\theta)_{mean}}{u_{mean}} \tag{10}$$

Using Eqs. 10, the Nusselt number can be obtained for the case of one side wall heated or all walls heated, using the corresponding θ profiles. The computed Nusselt Number for one side wall heating case is shown in Fig. 6. It is easily ascertained from Fig. 6 that the Nusselt Number approaches an asymptotic value as Hartmann number increases. These asymptotic values depend on the aspect ratio of the channel and are given in Table 1. It is also seen in Fig. 6 that as $H \to 0$, the computed Nusselt Numbers agree very accurately with their hydrodynamic limits as given in literature [2, 3]. In Table 1, we also give the computed value of Nusselt number for the all walls heated case for purpose of comparison.

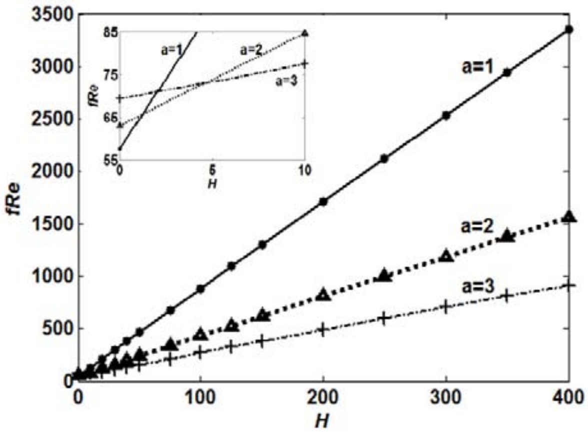

Fig. 5 Plot of fRe as a function of H

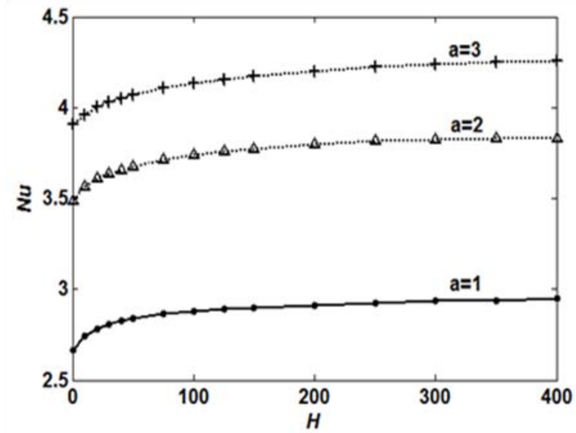

Fig. 6 Plot of Nu as a function of H

Table 1 The factor χ in Equation 8 and Nu for an electrically insulated rectangular channel

Aspect ratio, a	χ	Nu (one side wall heated)	Nu (all walls heated)
1	8.446	2.934	6.55
2	3.960	3.823	6.70
3	2.355	4.241	6.73

5. A Parametric Study of Heat Extraction from the First Wall

Using the friction factor and the Nusselt numbers calculated in the preceding section, a simplified parametric feasibility study of cooling the first wall with liquid metal flows is performed in this section. This study is valid for electrically insulated ducts with one of the side walls of the duct in thermal contact with the first wall. We consider here the three prime candidates for self-cooled liquid metal breeding blankets, i.e., lithium, lead-lithium, and tin-lithium alloys. Their composition and properties are listed in Table 2 [7]. The hydrodynamic, thermal and electrical properties of these liquid metals vary over a wide range. Our purpose is to identify those groups of properties which determine the suitability of these for heat removal from the first wall, and also to identify the scaling laws for duct dimensions (Y_0, Z_0), dynamic pressure drop Δp, and the heat removal rate (HR) to pumping power (PP) ratio, which are the key considerations from the view point of thermal-hydraulic design of such a cooling system and its impact on the overall thermal efficiency of the fusion power plants. Towards this purpose, we consider the parameters given in Table 3 to be the input/specified design parameters. A set of reference values is also given in Table 3.

Table 2 Thermophysical properties of different liquid metal coolants

Property	Unit	Lithium (100%)	Lead-Lithium (83%Pb,17%Li)	Tin-Lithium (80%Sn,20%Li)
ρ	$\mathrm{kg.m^{-3}}$	4.90×10^2	9.20×10^3	6.80×10^3
c_p	$J.kg^{-1}.K^{-1}$	4.15×10^3	1.89×10^2	3.17×10^2
k	$W.m^{-1}.K^{-1}$	43.49	16.12	33.44
σ	$A.V^{-1}.m^{-1}$	2.90×10^6	7.50×10^5	1.67×10^6
ν	$m^2.s^{-1}$	7.10×10^{-7}	1.40×10^{-7}	1.77×10^{-7}
$\sqrt{(\sigma\nu/\rho)}\,/\,k^2 c_p$ *	$m.s.K^3.W^{-2}.T^{-1}$	8.25×10^{-9}	6.88×10^{-8}	1.86×10^{-8}
$\rho k^2 c_p^2 \sqrt{(\rho/\sigma\nu)}$ **	$T.W^3.m^{-4}K^{-4}$	2.47×10^{14}	2.52×10^{13}	1.16×10^{14}

*A material property on which Δp depends (see Eq. 17)
** A material property on which HR/PP depends (see Eq. 18)

Table 3 Input Parameters and their reference values

Parameter	Unit	Description	Reference value
a	$-$	Channel aspect ratio	1 to 3
q	$MW.m^{-2}$	Heat flux from the first wall	1
B	T	Magnetic field transverse to the coolant flow	5
L	m	Length of the coolant channels with transverse magnetic field	5
ΔT_c	K	Temperature rise in the coolant from inlet to exit	200
ΔT_w	K	Temperature drop from first wall to the liquid metal coolant	100
$(Bq^3 L^2)/(\Delta T_c\,\Delta T_w^2)$	$T.MW^3.m^{-4}.K^{-3}$	Combination of input parameters on which Δp depends (Eq. 17)	62.50×10^{-6}
$(Bq^3 L^2)/(\Delta T_c^2\,\Delta T_w^2)$	$T.MW^3.m^{-4}.K^{-4}$	Combination of input parameters on which HR/PP depends (Eq. 18)	31.25×10^{-8}

5.1 Governing Thermal-Hydraulic Relations

Convective heat transfer from the first wall

$$q = h(T_s - T_{mean}) = h\Delta T_w \tag{11}$$

where symbols are as defined earlier and also given in the Nomenclature.

Dynamic pressure drop

$$\Delta p = f \frac{1}{2} \rho v_{mean}^2 \frac{L}{D} \tag{12}$$

Pumping power

$$PP = \dot{Q} \Delta p = \frac{\dot{m}}{\rho} \Delta p \tag{13}$$

where the volumetric flow rate, $\dot{Q} = 4Y_0 Z_0 v_{mean}$,

Heat removal rate (HR) from the first wall

$$HR = q2Y_0L = \dot{m} c_p \Delta T_c \tag{14}$$

As mentioned earlier, the ratio of heat removal rate to pumping power is an important figure of merit for the first wall cooling system. Using Eqs. 11-14, this ratio can be expressed in the following dimensionless form:

$$\frac{HR}{PP} = \left(\frac{4a}{1+a}\right) \frac{Nu}{Pr.fRe.Ec} \tag{15}$$

where Pr is the Prandtl number and Ec is the Eckert number (see Nomenclature). The Nusselt number depends on the aspect ratio a of the cooling channel and fRe depends on the aspect ratio and the Hartmann number as given in Table 1.

5.2 Explicit Solutions of Thermal-Hydraulic Relations for Critical Variables

The thermal-hydraulic relations expressed in Eqs. 11-15, together with Eq. 8 and the values given in Table 1, the material properties listed in Table 2, and the input design parameters given in Table 3, determine implicitly the cooling channel dimensions (Y_0, Z_0), the dynamic pressure drop (Δp), and the heat removal rate to pumping power ratio (HR/PP). However from these relations, their dependence/scaling with respect to the input parameters of Table 3 is not obvious. It is worth the algebraic effort to obtain the dependence of these critical variables on the specified parameters given in Table 3. After straight but somewhat lengthy manipulations, these relations can be obtained as given below:

$$Y_0 = \left(\frac{1+a}{4}\right) Nu * k * \frac{\Delta T_w}{q} \tag{16}$$

$$\Delta p = \frac{a\chi}{4Nu^2} * \frac{1}{c_p k^2} \sqrt{\frac{\sigma \nu}{\rho}} * \frac{Bq^3L^2}{\Delta T_c \Delta T_w^2} \tag{17}$$

$$\frac{HR}{PP} = \frac{4Nu^2}{a\chi} * \rho k^2 c_p^2 \sqrt{\frac{\rho}{\sigma \nu}} * \frac{\Delta T_w^2 \Delta T_c^2}{Bq^3L^2} \tag{18}$$

The channel dimensions are considered as a critical variable because the hydraulic diameter of the channel can become impractically small to achieve adequate convective heat transfer coefficient. The dynamic pressure drop (together with the static head) should be as small as possible for low pressure operation and is thus an important variable. Finally, the heat removal rate to pumping power ratio should be as large as possible for better thermal efficiency of the fusion power plant.

5.3 Results and Discussion

Important parametric trends can easily be ascertained from Eqs. $16 - 18$. The right hand side in each of these equations can be regarded as a product of three factors:

- **(a)** The first factor depends only on the channel aspect ratio a including the dependence of χ and Nu on a, as given in Table 1.
- **(b)** The second factor in these equations depends only on a particular property or combination of properties of the liquid metals listed in Table 2.
- **(c)** The third factor depends on a particular combination of the specified input design parameter listed in Table 3.

The parametric dependence of the selected variables on a particular material property or input design parameter is easily seen in these equations. For example, the dynamic pressure drop is inversely proportional to the square of the thermal conductivity and increases in proportion to cube of the heat flux from the first wall. As an another example, the ratio of heat removal to pumping power improves quadratically with respect to the product $\Delta T_c \Delta T_w$.

In Figs. $7-9$ we give some plots for the critical variables with respect to the third factor (depending uniquely on the selected design parameters) for different materials and channel aspect ratios.

It may be mentioned here that Eqs. $16 - 18$, on which these graphs are based, are valid for channels with insulating coatings. The wall conductance may enhance the Nusselt number due to high velocity jets developing on the side walls of the channel. This will have a beneficial effect on the critical performance variables. However, the scaling of fRe with respect to Hartmann number becomes worse in the case of conducting walls due to induced currents in the channels walls. This will change the scaling of Δp and HR/PP, in particular, with respect to the magnetic field/Hartmann number.

Other variables of interest (for example v_{mean} , $Re,$ etc) are easily ascertained from the thermal hydraulic relations given in Eqs. 11-14, and we have not given here their explicit dependence on input parameters. In Table 4, we show some of these variables corresponding to the reference values of Table 3 for square channels ($a = 1$).

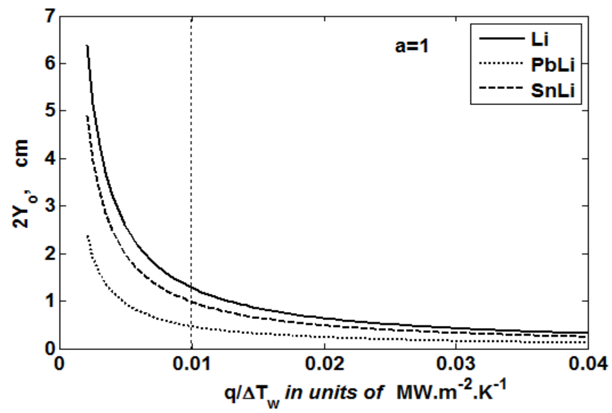

Fig. 7 Plot of channel width $2Y_0$ as a function of input parameters for different liquid metals for a square channel

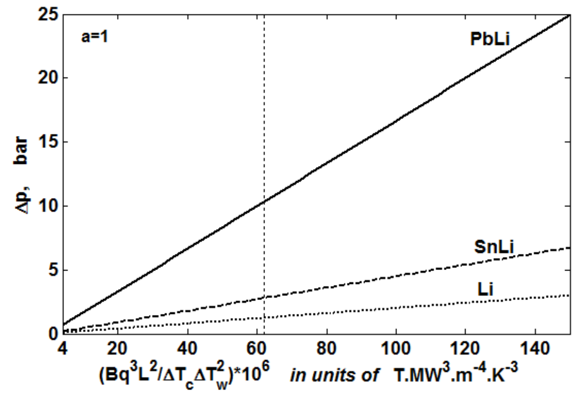

Fig. 8 Plot of pressure drop Δp as a function of input parameters for different liquid metals for a square channel

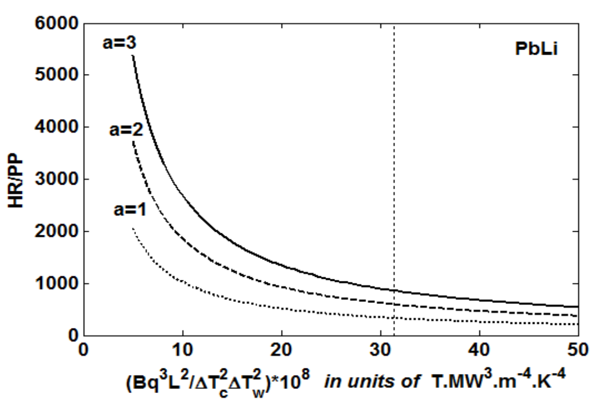

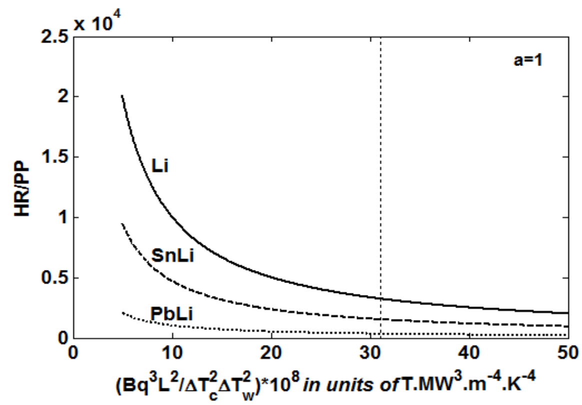

Fig. 9 Plot of heat removal rate to pumping power ratio (HR/PP) as a function of input parameters for different channel aspect ratios (left) and different liquid metals (right)

Table 4 Output variables of interest for reference input values for a square channel (a=1)

Output variables	unit	Li	Pb Li	Sn Li
$2Y_0$	mm	12.8	4.8	9.8
v_{mean}	ms^{-1}	0.96	3.04	1.18
fRe	$-$	24600	2410	7730
Re	$-$	17300	102800	65700
H	$-$	2913	285	915
ΔP	bar	1.25	10.4	2.81
HR/PP	$-$	3217	329	1514

It can be seen from Fig. 7 that due to higher thermal conductivity, the duct dimensions required to cool the first wall are most favorable for Li, as implied by Eq. 16. Similarly, the crucial material property, $(\sqrt{\sigma\nu/\rho})/(c_p\, k^2)$, which determines the dynamic pressure drop (see Eq. 17) is most favorable for Li, followed by SnLi and PbLi (see Table 2). The heat removal rate to pumping power ratio ($/PP$) is determined by the material property, , $\rho k^2 c_p^2\sqrt{\rho/\sigma\nu}$ (see Eq. 18). As can be seen from Table 2, this property is about 10 times better for Li than for PbLi and about twice better as compared to SnLi. We may also mention here that making side walls of the rectangular channel larger than Hartmann walls ($a > 1$) has a favorable effect on both Δp and HR/PP.

6. Conclusion

Based on the analysis and the computational results presented in this work, the cooling capability of the first wall by liquid metals appears to be feasible, allowing the simplicity of self-cooled breeder blankets. From the thermal-hydraulic viewpoint, lithium appears to be the best, allowing largest cross-sectional dimensions of the ducts for the first wall heat extraction, lowest pressure operation, and yielding highest heat removal rate to pumping power ratio. Explicit scaling laws for these performance parameters with respect to material properties and input design variables such as heat flux at the first wall, magnetic field, channel length and aspect ratio, allowable temperature rise in the coolant from inlet to exit, and temperature drop from first wall to coolant, are given for channels with insulating coatings.

Nomenclature

a channel aspect ratio (Fig. 1)
b dimensionless induced magnetic field
$\boldsymbol{B_0}$ applied magnetic field
$\boldsymbol{B}$ net magnetic field
c_p specific heat capacity
D hydraulic diameter
Ec Eckert number, $v_{mean}^2/c_p\Delta T_w$
f friction factor
h convective heat transfer coefficient
H Hartmann number, $Y_0 B\sqrt{(\sigma/\rho\nu)}$
HR heat removal rate from the first wall
k thermal conductivity
L length of the coolant channel
Nu Nusselt number
p pressure
PP pumping power
Pr Prandtl number, $k/\mu c_p$
q heat flux at the first wall
Re Reynolds number, vD/ν
Rm magnetic Reynolds number
T temperature
T_s surface temperature of the first wall
u dimensionless speed
v speed of flow
y Y/Y_0 (Fig. 1)
z Z/Z_0 (Fig. 1)
ΔT_c see Table 3
ΔT_w see Table 3
θ dimensionless temperature
χ see Eq. 8 and Table 1
ρ mass density
σ electrical conductivity
ν kinematic viscocity

References

[1] U. Muller and L. Buhler, "Magnetohydrodynamics in Channels and Containers", Springer, 2001.

[2] F.P. Incropera and D. P. Dewitt, "Fundamentals of Heat and Mass Transfer", John Wiley & Sons, New york, 1996.

[3] T. F. Irvine, Jr. and James P. Hartnett, "Advances in Heat Transfer", Academic Press, 1978.

[4] D. E. Fussy, " *MHD duct flows at moderate Hartmann number*", J. Phys. D: Appl. Phys., 1971,Vol. 4.,1929-1939.

[5] J. H. Mathews and K. D. Fink, "Numerical Methods Using Matlab", 1999.

[6] S. C. Chapra and R. P. Canale, "Numerical Methods for Engineers", Tata McGraw-Hill, 2008.

[7] Thick Liquid Blanket Concept, APEX Interim Report, November 1999.